Nasa CR 65413 Manry

GPO PRICE $ ______

CFSTI PRICE(S) $ ______

Hard copy (HC) $2.00

Microfiche (MF) .50

ff 653 July 65

TRW SYSTEMS

ONE SPACE PARK • REDONDO BEACH, CALIFORNIA

N66 30116 (ACCESSION NUMBER)

(THRU)

47 (PAGES)

1 (CODE)

CR-65413 (NASA CR OR TMX OR AD NUMBER)

23 (CATEGORY)

FACILITY FORM 602

DEVELOPMENT AND FABRICATION OF ABLATIVE OPTICAL BEACONS

FINAL REPORT

CONTRACT NAS 9-5374

5541-6001-R0000

17 May 1966

Prepared for

National Aeronautics and Space Administration
Manned Spacecraft Center
Houston, Texas

Prepared by
F. N. Mastrup
Project Engineer

Approved by
D. L. Cronin
Project Manager

R. Odenberg
Project Engineer

A. D. Schoenfeld
Manager, Power
Systems and
Conditioning Dept.

TRW SYSTEMS

CONTENTS

ILLUSTRATIONS

1. INTRODUCTION

1.1 GENERAL

This final report was prepared by TRW Systems for the National Aeronautics and Space Administration, Manned Spacecraft Center, under Contract NAS9-5374, "Development and Fabrication of Ablative Optical Beacons". The work covered by this report was performed between 4 December 1965 and 30 April 1966.

1.2 BACKGROUND INFORMATION

Ultimately, it is planned to install an optical beacon, of some as yet to be determined type, aboard the Apollo Command Service Module. Such a beacon would provide a visual reference point for crew members in the Lunar Excursion Module. The effort reported here was undertaken to demonstrate the life, reliability and spectrum of radiation of the TRW ablative flash lamp, with particular consideration given to its performance in the space environment and suitability for the Apollo mission. To meet these goals, a program was initiated which included the design, fabrication and testing of prototype lamps and the fabrication and delivery of six of the two best lamp designs.

Prior to this contract award, TRW had completed a great deal of development work on methods of light radiation employing ablative principles. Two patent applications, Numbers 325085 and 327388, are pending and lamps of very high Joule levels are being used in practical hardware applications. In many of these applications the plastic ablative, self-filling light sources have demonstrated superior characteristics over conventional gaseous discharge light sources. Much of the technical data made available to the effort was based on the results of TRW's independent R&D programs, such as a prior investigation of the phenomenon of very high Joule level flashes at low repetition rates. In such applications the average heating effect was low and well within the temperature capabilities of the ablative material used (plexiglas). Consequently, material studies have been concentrated on plexiglas, and investigations of other materials, including quartz, had not been pursued in depth. However, the repetition rates and

Joule levels required in this development established the level of average power dissipated in the lamp at approximately 135 w. This requirement imposed two new design conditions:

1) The section of the lamp containing the main gas discharge must be made of very high temperature materials

2) Since the ablative material source (usually a plastic or polymer structure) has a fairly low temperature rating, it must be thermally isolated from the main lamp section.

To meet the high temperature requirement in the main light chamber, quartz was selected as the material of construction. To solve the second problem, thermal isolation of the source of ablative material, two approaches were explored. In the first, a boiler initiates the ablative process. In the second (called a pulsed ablator) a small plastic lamp operates independently of the main chamber but exhausts its discharge gases through the main chamber. Both of these approaches proved feasible and are discussed in the report.

At the start of the effort TRW believed that the temperature problems associated with the ablative lamp were less severe than those associated with Xenon lamps. Significantly, the analytical comparison made between Xenon and ablative type lamps confirmed this hypothesis.

1.3 WORK ACCOMPLISHED

As required in the Statement of Work for Contract NAS9-5374, TRW has accomplished the following:

1.3.1 Design

Two ablative lamp designs were completed; both lamp designs when optimized had essentially the same final physical configuration. The two required designs were:

- Design No. 1 — 7.5 Joules input, 32 flashes/sec
- Design No. 2 — 240 Joules input, 1 flash/sec

In addition to fulfilling the contractually required design effort, TRW also investigated an ablative lamp concept which employed a different triggering principle. This concept also demonstrated a capability for meeting the specified design goals.

1.3.2 Hardware Fabrication

1) Prototypes. Four prototype lamps of Designs 1 and 2 were built and tested for color temperature and lamp efficiency. In addition, a prototype of the pulsed ablator lamp was also built.

2) Deliverable Lamps. Twelve final configuration lamps have been built in accordance with the contractual schedule requirements.

3) Power Supply Breadboards. Power supply breadboards have been built for each type lamp. The circuit configuration of the power supply design was based on the use of laboratory equipment.

1.3.3 Test Program

The final configuration boiler ablative lamp design was subjected to the following tests:

1) Radiated spectral distribution
2) Total radiated energy
3) Efficiency tests
4) Life tests (including restart capability)
5) Exhaust gas thrust phenomena.

1.3.4 Environmental Testing

Thermal vacuum tests were conducted with the lamp reaching an operating temperature of 1,000^{o}F.

1.3.5 Comparative Study of Xenon and Ablative Lamp Concepts

The results of this study are described in the body of the report.

1.4 CONCLUSIONS

The ablative lamps developed and supplied under this contract are competitive with or exceed the performance capabilities of Xenon lamps in many applications. In particular, the ablative flash lamp is far superior when high Joule applications are required. The specific operating conditions for which the ablative lamp is best suited are typified by:

1) Short flash duration
2) Very high peak intensity
3) Vacuum environment
4) High average wattage dissipation
5) Ultraviolet light output
6) Constant light intensity with each flash over long periods of time.

The two trigger systems which were mechanized, pulsed ablator and boiler, showed equal promise initially, but the boiler approach was selected for this application.

The laboratory power supplies used for this program will have to be adapted to the space environment for the flight qualified units.

During the design and evaluation stages of the effort, it was found that the quartz walls of the main chamber were ablating. This phenomenon suggested that several approaches to the triggering concept and power supply were feasible, and that the circuit design would, to a large extent, be influenced by the particular application. The approach to the power supply and circuitry which was used was adequate for the lamp evaluation required here, and can subsequently be optimized for a specific application.

Quartz proved to be an excellent ablator for this type of lamp, with advantages in thermal capability and in inherent transmission of ultraviolet light. Efficiencies of 28 percent were attained with measured radiation limited to between 0.355 and 1.1 μ. If this spectrum were extended to shorter wavelengths, even higher efficiencies of up to 50 percent are anticipated.

Two major operating characteristics clearly demonstrated in the test results show the superiority of the ablative lamp:

1) No degradation of light output with operating life. This is possible because, unlike Xenon, the ablative lamp exhausts any tube-darkening material after each flash. Also, the ablative process wipes the wall of the tube clean so that each flash then can start with a clean quartz wall.

2) The light intensity of each flash is nearly exactly the same.

To the application engineer these features are important in that the system rating (power supply and power source) is established by the minimum light requirement at end of mission life. The savings in weight and system efficiency are obvious when one one considers that Xenon is rated at 50 percent of initial light output at 10,000 flashes, and varies in intensity as much as 30 percent from flash-to-flash.

The rate of ablation of the quartz walls was found to be very dependent on the quality of quartz. Tests run with industrial quality quartz showed a very high consumption of the lamp inner wall, but optical quality quartz had a very nominal burning rate with no degradation of efficiency.

Operating life and failure modes were restricted to the mechanical design of the anode electrode. With the new designs discussed in the report, operating life could be radically extended.

Two failure modes experienced were attributed to the electrode design. One failure was caused as the anode electrode burned away after 22 hours of operation. This can be corrected by a change in electrode size and length. The second failure was caused by the use of an oversized electrode; longer electrode life was achieved but such a low operating temperature resulted that the by-products of the ablation process, SiO_2, condensed on the anode. The condensation formed an insulating layer which stopped the electrical discharge during life tests. The lamp that failed in this mode was restored to an operational state simply by scraping off the quartz desposit. Mechanical designs of an anode which would eliminate these two problems are discussed in the body of the report.

2. TECHNICAL DISCUSSION

2.1 INTRODUCTION

This section discusses the technical details of the program, the tests which were performed, the analytical data which were generated, and the design features of the ablative lamps. The discussion is organized under two major subdivisions, "2.2 Boiler Concept" and "2.3 Pulsed-Ablator Concept". Subsection 2.2 presents a description of the data relative to the two contractually required designs. Subsection 2.3 discusses, in somewhat lesser detail, key points of the preliminary investigation of the pulsed-ablator concept.

2.2 BOILER CONCEPT

2.2.1 General

Specific design goals of the program included the construction of lamps capable of 1 and 32 flashes per second repetition rates, 250-w average power input, and lamp life of 150 hour continuous operation. The lamps built during the program have been operated continuously in a high vacuum environment for periods of 22 hr at 250-w input power, and 10 hr at 500 w. At the indicated power levels, total radiative efficiencies of between 24 and 28 percent have been demonstrated. Lamps that became inoperative or inefficient after approximately 22 hr were inspected and found to have developed problems of a minor nature. Specifically, no physical damage to the lamp structure was observed. This finding opens the way for the construction of compact lamps capable of operating in a hard vacuum environment at average continuous input power levels of 500 w or higher for up to 10^6 flashes. Radiative efficiencies can be expected between 20 and 30 percent. The lamp structure would be cooled solely by radiation with no cooling fluid or heat-sinks required.

2.2.2 Functional Description

The TRW-developed, boiler ablative lamp concept makes possible a high-intensity flash lamp which eliminates the need for a sealed glass or quartz tube and a permanent gas filling. The principle of operation is to employ the heat generated by an electrical discharge to ablate and vaporize material from the quartz discharge-confining walls. This vaporized material then acts as the carrier gas for the flashing operation.

An electrical discharge through an ablating lamp consists of three phases: ignition, discharge, and exhaust. Ignition can be accomplished either by a gaseous breakdown or by a sliding spark in a high vacuum. The high-vacuum sliding spark ignition does not require any initial gas pressure, but does require contact between the electrodes and the lamp wall. Such contact causes problems when continuous operation for many flashes is required.

The ablating lamps described here are provided with a very low initial gas pressure of approximately 0.1 torr. During discharge, the gas pressure rises rapidly by many orders of magnitude above this initial pressure. Peak pressures of many atmospheres are common in similar lamps where this parameter has been measured. It has been found that the initial gas pressure of 0.1 torr, required for lamp ignition, can be obtained from outgassing of the hot lamp structure once the system has operated for a few flashes. The problem, therefore, is to devise a method of firing the lamp when the whole structure is quite cold. In the TRW lamp a 25-w boiler containing a small pellet of Plexiglas is connected to the lamp, via a heat insulating thin-walled stainless steel tube. This boiler is heated to approximately 125°C, which takes a few minutes in a vacuum environment, causing the Plexiglas pellet to outgas and thus provide the initial background pressure necessary for firing. After continous flashing operation has commenced, the boiler is shut off. The heat-insulating tube prevents the high temperatures in the main lamp structure from overheating the boiler.

The discharge phase in an ablating lamp differs from that in conventional prefilled lamps in several respects. The most significant difference is that in an ablating lamp there is a very strong interaction between the discharge-confining wall and the hot plasma. For example, during discharge, the ablated material causes a rapid increase in gas density. This, in conjunction with the normal rise in pressure which accompamies increasing temperature, produces an extraordinarily rapid and high pressure buildup in the ablating lamp. As a consequence, spectral emission from the Bremsstrahlung and bound-free continuums is much more dominant since the intensity of each depends on the square of the pressure. Also, the fact that the typical electron densities in ablating lamp plasmas are considerably higher than in ordinary lamps of comparable design results in significant line-broadening. Consequently, the spectral energy distribution in ablating lamps is generally continuous.

The third phase is the exhaust of the gases which have been ablated and heated in the lamp during the discharge phase. Proper means have to be provided to exhaust these gases, with particular attention given with respect to the condensability of the exhaust gas products. An ablative quartz lamp has exhaust gas products including Si, SiO, SiO_2, and O_2. Of these, the first three are highly condensable and are easily accumulated in a suitable space provided at the end of the lamp. The small amount of gaseous oxygen produced by the discharge is bled out of the lamp through ports. Additional exhaust gas products resulting from electrode erosion are also highly condensable.

Heat transfer and heat exchange are of great importance for any lamp designed to operate in a hard vacuum environment. Of primary concern is the removal of heat from the discharge-confining quartz structure, mainly because only a very small portion of the excess heat can be disposed of by conduction along the quartz tube. Also, since no convective medium for cooling is available, the only effective means available for removing excess heat is radiative cooling. Consider a lamp structure consisting of two electrodes and a long quartz tube of outside radius R_o and inside radius R_1. The average power balance equation is as follows.

$$P_{ab} + P_{AN} + P_{CA} + P_{ex} + P_{or} + P_{hr} = P_{el} \quad (1)$$

where

P_{ab} = average power dissipation in ablation

P_{AN} = average power dissipation in the anode

P_{CA} = average power dissipation in the cathode

P_{ex} = exhaust enthalpy flow

P_{or} = average optical radiation power

P_{hr} = average heat radiation from the quartz tube

P_{el} = average electrical input power

Approximate values for the different terms are:

$$P_{AN} + P_{CA} \approx 20 \leftrightarrow 30 \text{ percent}$$

$$P_{or} \approx 20 \leftrightarrow 30 \text{ percent}$$

$$P_{ex} \approx 15 \leftrightarrow 25 \text{ percent}$$

$$P_{ab} \approx 20 \leftrightarrow 30 \text{ percent}$$

$$P_{hr} \approx 2 \leftrightarrow 7 \text{ percent}$$

The relative sizes of the various terms in the heat balance equation can be considerably influenced by the characteristics of the ablative lamp design.

From the above it is seen that exhaust gas enthalpy and ablation combine to remove approximately 45 percent of the total dissipated energy from the quartz structure. This is a decisive point when high-power operation in a vacuum is required. A relatively small amount of heat will remain in the discharge-confining quartz tube. It is this residual heat ($\approx$ 5 percent of the total) which is of greatest concern.

The limitation on using conduction to remove heat from the quartz tube is illustrated in the following calculation. Consider a quartz tube of 9 mm O. D. and 3 mm I. D.; cross-sectional area is 0.566 sq cm, thermal conductivity (λ) of quartz is 1.8×10^{-2} w/cm^{o}K for material at 400^{o}C. Heat flow supported by a heat gradient of 100^{o}K/cm is:

$$\dot{Q} = -\lambda A \frac{dT}{dx} = 1.8 \times 10^{-2} \times 0.566 \times 10^{2} = 1 \text{ w} \tag{2}$$

In an elongated quartz tube, heat gradients are expected to be much less than 100^{o}K/cm, except at the ends where the quartz contacts metallic support structures. Thus, the sole remaining mechanism for removing heat from most of the quartz tube is radiation. Let Q' be the heat/cm of length transferred to the quartz tube. Then

$$Q' = \frac{P_{hr}}{\ell} \text{ w/cm}$$

where

$$\ell = \text{lamp length} \tag{3}$$

Let r be the variable radius. Heat balance requires

$$Q' = -\lambda 2\pi r \frac{dT}{dr} \text{ w/cm}$$

and (4)

$$Q' = \varepsilon(T)\sigma 2\pi \, r_o \, T_o^{\,4} \text{ w/cm}$$

where

$\varepsilon(T)$ is the temperature-dependent quartz emissivity

σ is 5.67×10^{-12} w/cm^2(^{o}K)^4

T_o is the temperature of the quartz tube's outside wall

The solution for the difference between the inside wall temperature T_i and the outside wall temperature T_o is

$$T_i - T_o = \left(\frac{Q'}{2\pi\lambda}\right)\left(\ln\frac{r_o}{r_i}\right) \tag{5}$$

For the temperature ratio one finds

$$\frac{T_o}{T_i} = 1 - \frac{Q'}{2\pi\lambda_1} \ln\frac{r_o}{r_i} = 1 - A \ln x \tag{6}$$

where

$$x = \frac{r_o}{r_i}$$

$$A = \frac{Q'}{2\pi\lambda_1}$$

A numerical example will show that the quartz tube temperature is virtually equal throughout the wall thickness. For the above example it is

$$Q' = \left(\frac{P_{hr}}{1}\right)\left(\frac{5 \times 10^{-2} \times 5 \times 10^{2}}{20}\right) = 1.25 \text{ w/cm} \tag{7}$$

where

$$A = \frac{1.25}{6.28 \times 1.8 \times 10^{-2} \times 8 \times 10^{2}} = 1.38 \times 10^{-2} \qquad (8)$$

where

$$r_i = 0.15 \text{ cm}; \ \lambda = 1.8 \times 10^{-2} \text{ w/cm}^{o}\text{K}; \text{ and } T_i = 800^{o}\text{K} ,$$

An outside wall temperature drop of 1 percent is expected when

$$\ell nx \approx 0.725 \longrightarrow x = \frac{r_o}{r_i} \approx 2.1 \qquad (9)$$

and of 10 percent for

$$\ell nx \approx 7.25 \longrightarrow x = \frac{r_o}{r_i} \approx 1,400$$

To satisfy the heat balance it is, therefore, only required to satisfy

$$r_o \geq \frac{0'}{2\pi\varepsilon\sigma T_o^{4}} \qquad (10)$$

Using $\varepsilon \approx 1$ one finds, for the same example

$$r_o \geq \frac{1.25}{6.28 \times 5.67 \times 10^{-12} \times (0.8)^{4} \times 10^{10}} = 0.084 \qquad (11)$$

This condition is automatically satisfied; but it is also realized that larger power inputs will rapidly increase the demands on outside tube radius. For example, it is hardly practical to choose $r_o > 0.4$ cm. Therefore, a power input above 6 w/cm can only be compensated for by increasing tube temperature beyond 800^{o}K. It is one of the advantages of the ablating lamp concept that this is possible. In fact, temperatures on the order of $1,000^{o}$K are altogether practical. By using tube diameters on the order of 0.8 cm, and operating temperatures of around $1,000^{o}$K, it is possible to radiate heat on the order of 20w/cm from the lamp structure. The possible power input for such a lamp is well into the kw-range. Figure 1 is a schematic of the TRW Boiler Ablative Lamp concept and associated circuits.

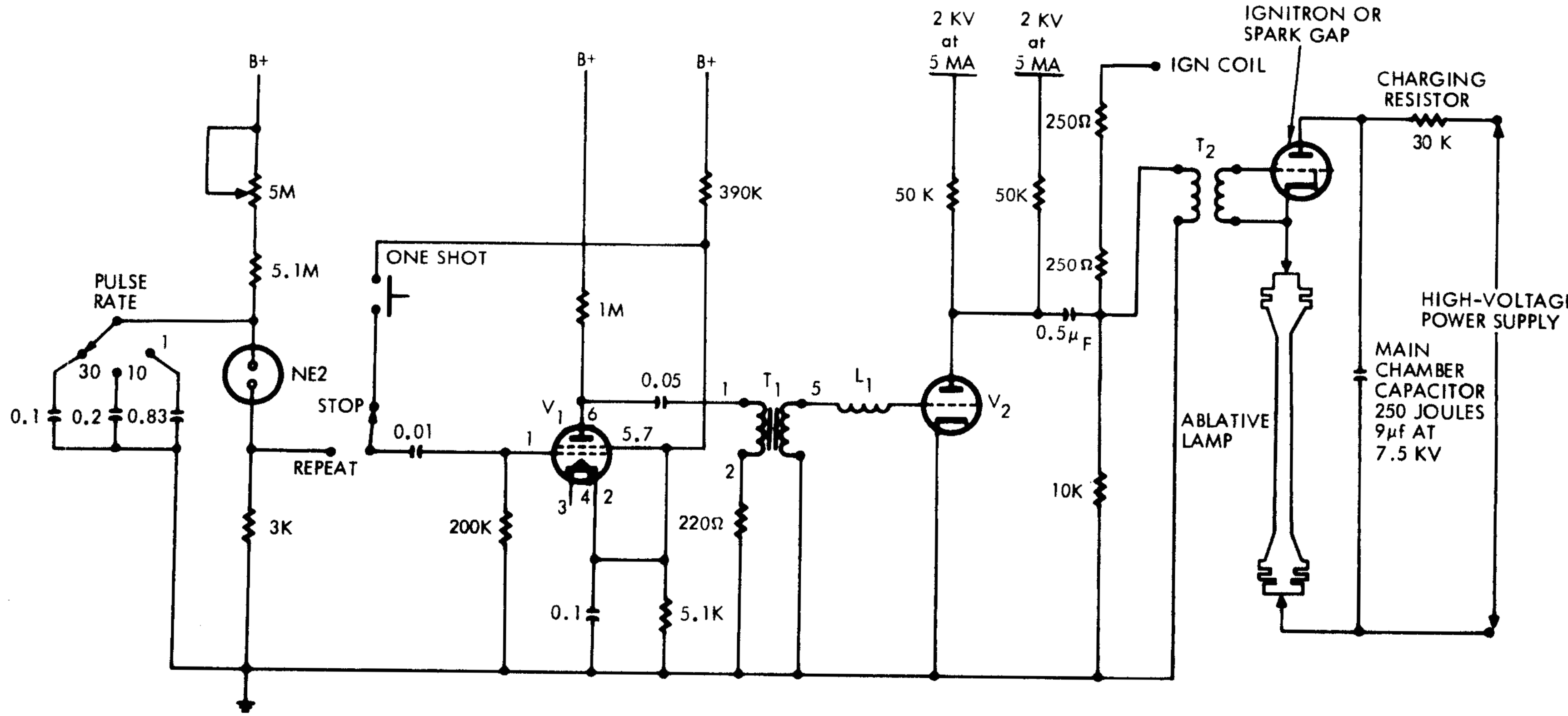

Figure 1. Schematic of Boiler Lamp Concept and Associated Circuitry

2.2.3 Design Features

A fully assembled boiler ablative lamp is shown in Figure 2. The quartz discharge tube is outfitted with conical ground quartz joints at each end. Conically shaped electrodes match the quartz cones to form the seal. To assure sufficient structural stability high tension copper-beryllium springs are used to hold the electrodes firmly in place. The lamp's present temperature limitation is a function of the annealing temperature of the copper-beryllium alloy. The ablated gas products exhaust through the tubular electrodes.

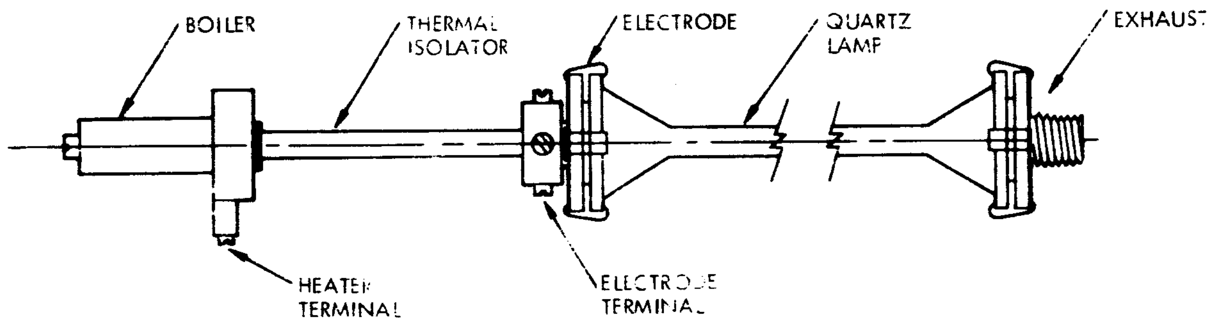

Figure 2. Fully Assembled Ablative Quartz Lamp

The lamp assembly allows thermal expansion of the electrode structure without damage to the quartz. Thus, it is possible to maintain sufficient sealing of the lamp up to very high temperatures. This is an advantage ablative lamps have over permanently sealed, prefilled gaseous discharge lamps. In the latter devices a perfect seal (usually a graded seal) has to be maintained at all times. In ablative lamps the less stringent sealing requirements permit the use of an imperfect seal such as that provided by a conical union where one member is allowed to expand freely.

Figure 3 shows a complete lamp assembly on a mounting fixture. The boiler which provides initial gas filling necessary for starting a cold lamp is also shown. Once the ablative lamp has flashed a few times, outgassing from the lamp walls eliminates any further need for boiler-supplied gas during an operational sequence. Approximately 25-w of power applied for a few minutes will heat the boiler to approximately 125°C, and cause adequate outgasing of the plexiglas pellet.

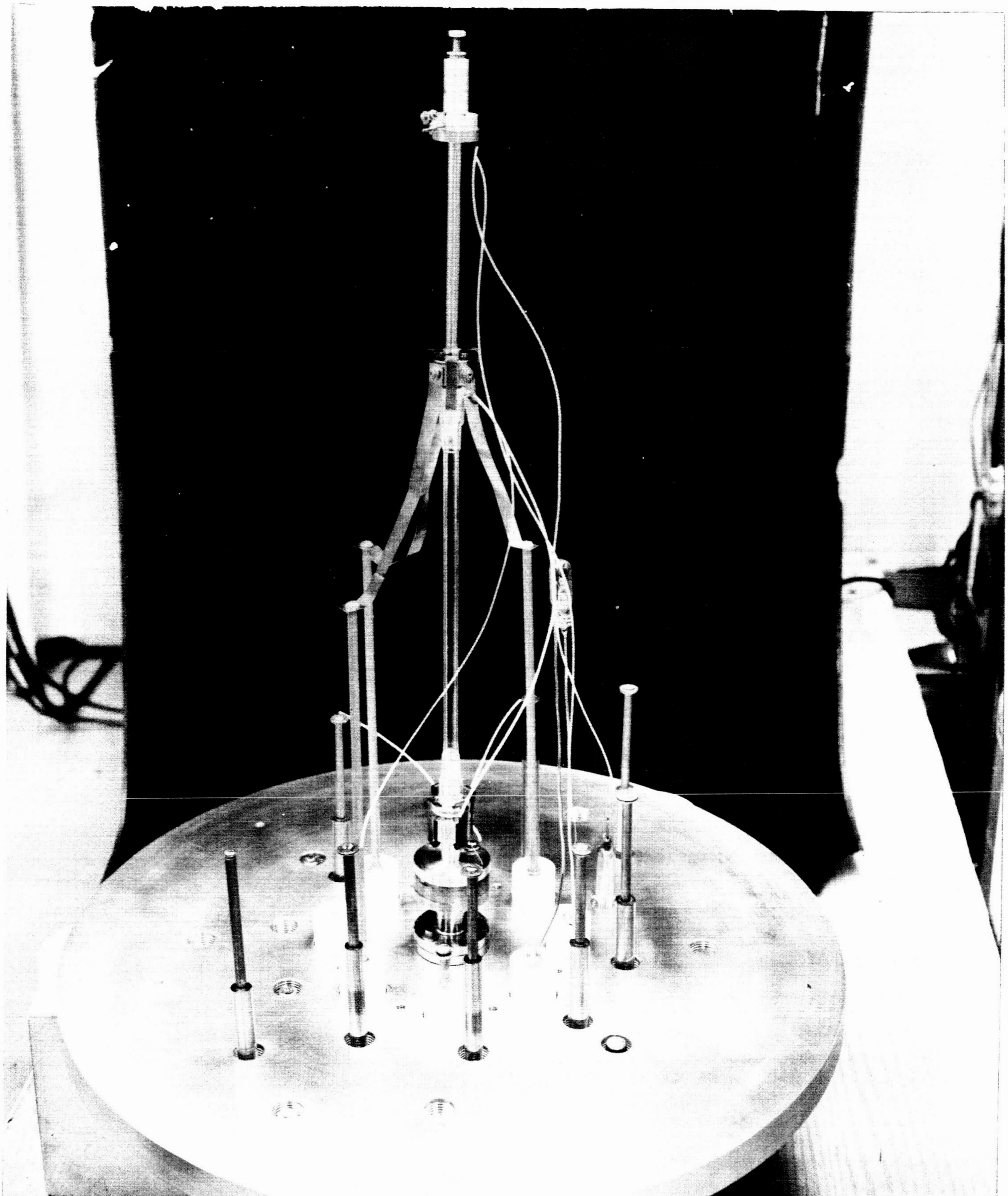

Figure 3. Lamp Assembly in Vacuum Fixture

2.2.4 Power Supply and Circuitry

During this program, extensive research was conducted to establish the optimum electrical circuit parameters. As a result, the circuits which are used make possible a total radiative lamp output at fixed input energy independent of circuit inductance or capacitance. This is only true, however, when the pulse length is less than 10^{-4} sec. The electrical discharge circuit used during most of the laboratory tests is shown in Figure 4.

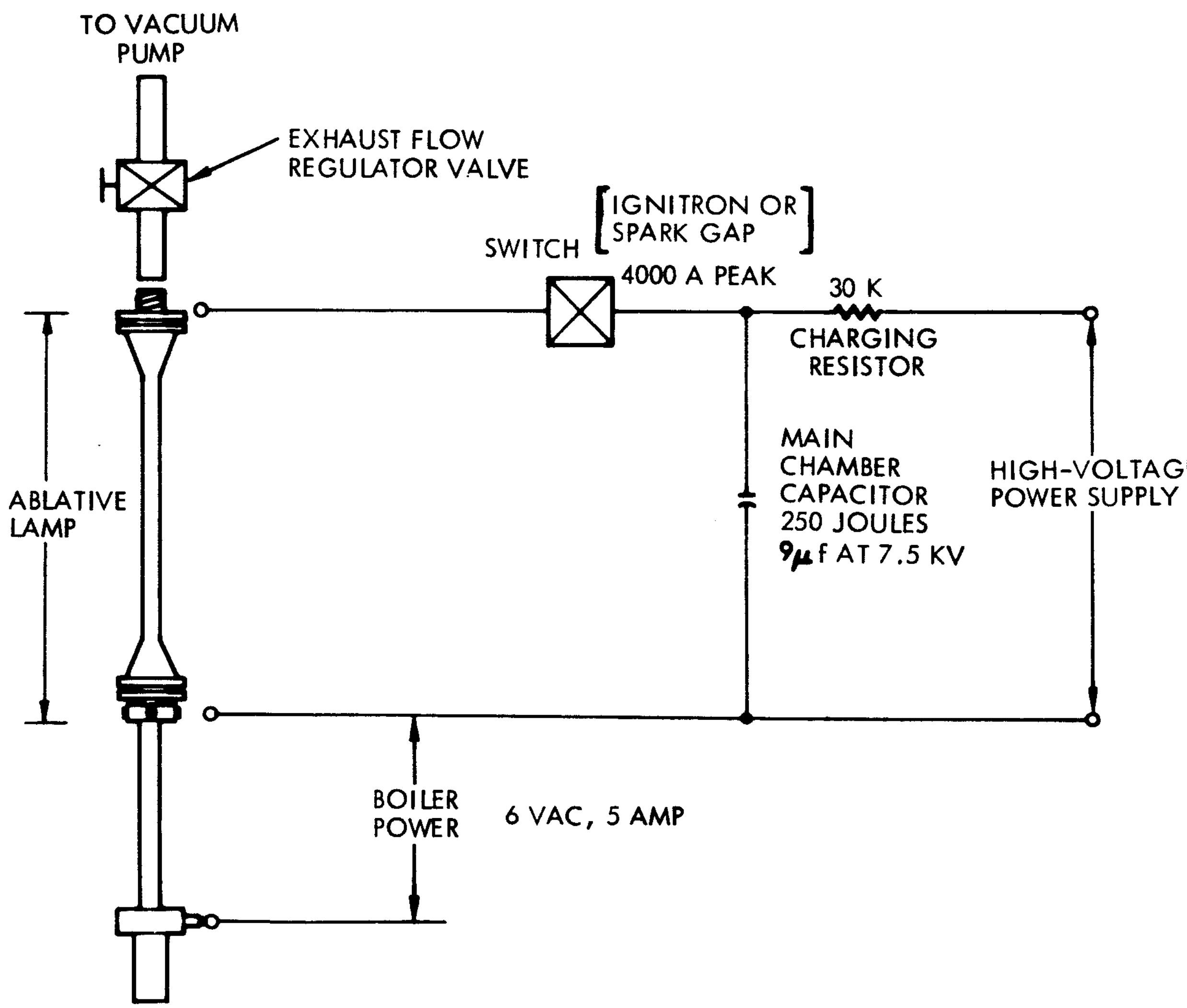

Figure 4. Diagram of Electrical Discharge Circuit

In the boiler method, power supplies and circuitry are needed for three primary functions.

1) Boiler heating
2) Triggering
3) Main chamber firing

2.2.4.1 Boiler Heating

A simple ohmic heating element, specifically Nichrome wire, is wound around the chamber containing the plexiglas pellet. In the test setup, the boiler temperature was controlled by manually varying the voltage to the heater winding. The voltage was 60-cycle ac, applied through a conventional 6 v filament transformer from a variable voltage transformer. After the lamp has been flashing for a short time, the boiler can be heated from the main burner. The heater power is then greatly reduced.

When the lamp is turned on, the boiler begins to heat. When the main chamber reaches operating temperature, it can supply most of the energy to heat the boiler. The electrical circuit may be disconnected at this time if continuous operation of the lamp is planned. The details of the circuitry are shown in Figure 5.

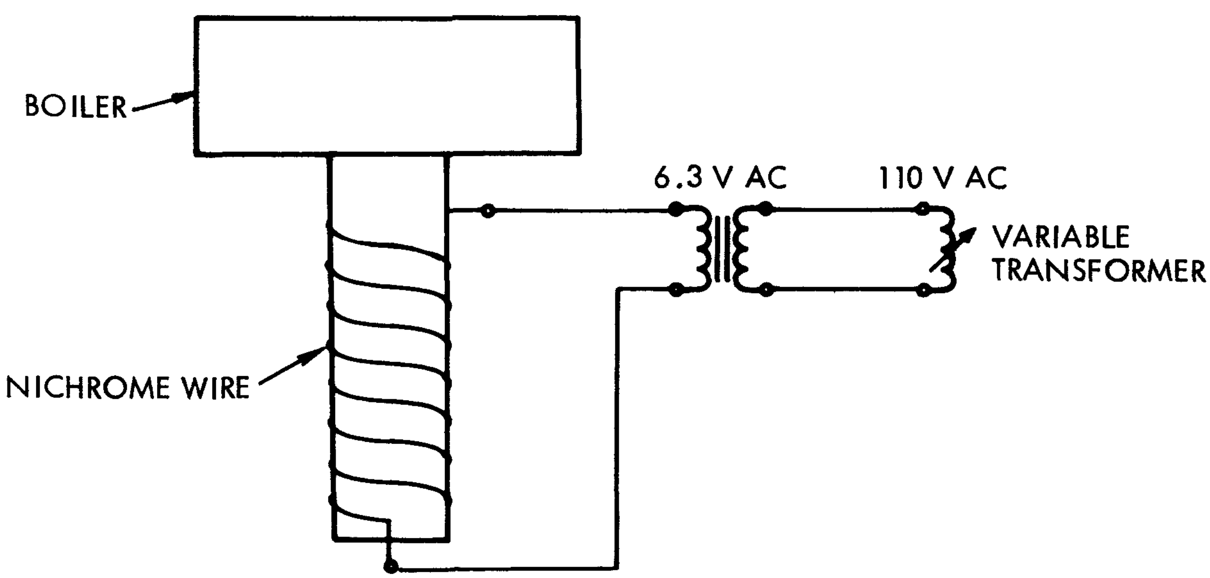

Figure 5. Boiler Heater Schematic

2.2.4.2 Triggering

A triggering circuit initiates the discharge in the main burner and also times the flash repetition rate. Two separate methods were used to switch the main chamber power. In one, an rf tickler coil surrounds the main chamber tube. In the other method, a series element Ignitron was placed between the main capacitor and the main burner electrodes. In both cases, the purpose of the trigger circuitry was to provide a short-duration, high-energy pulse. A block diagram of the trigger circuit is shown in Figure 6. In the test set-up, the Ignitron method proved to operate the best.

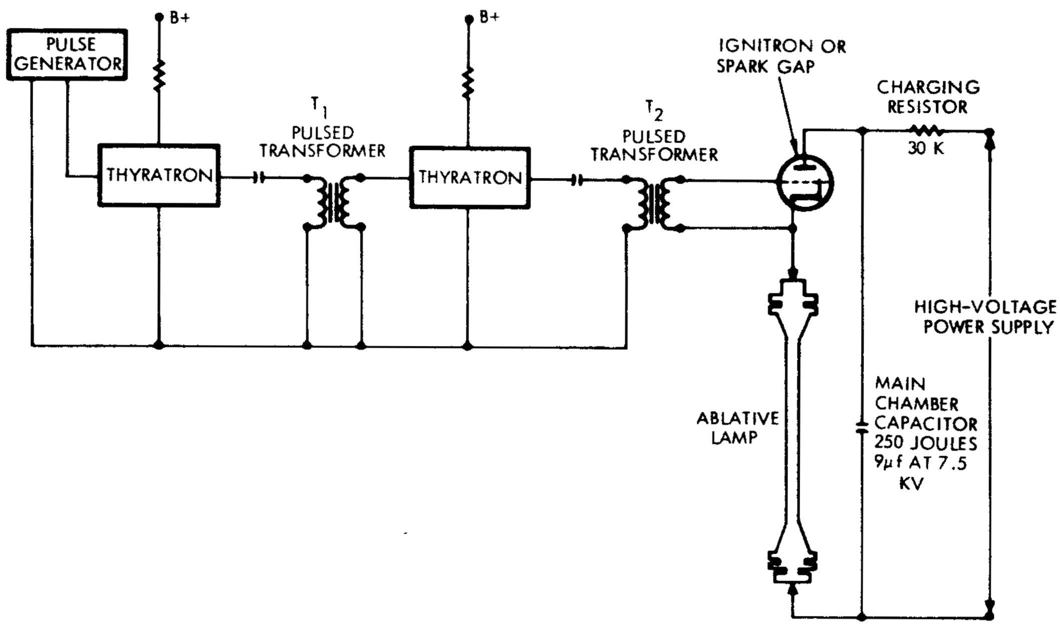

Figure 6. Block Diagram of Trigger Circuit

2.2.4.3 Main Chamber Firing

Main chamber firing is powered by an 8 kv dc, 400 w supply. It charges the main capacitor through a charging resistor. Details of the hook-up were shown in Figure 4.

2.2.5 Testing

2.2.5.1 Electrical Impedance, Power, and Light Pulse Shape

To determine the lamp impedance for the various quartz ablative lamp configurations, the discharge current and the voltage drop across the lamp were measured simultaneously as functions of time. Discharge current was determined with a Rogowski coil; the voltage drop was measured with a Tektronix capacitive potential difference probe. The two terminals were attached directly to the two electrodes to prevent circuit lead inductance from falsifying the voltage measurement. The ratios of the measured currents and voltages yield lamp impedance as a function of time; their product yields the lamp's instantaneous power consumption. Figure 7 shows current (upper trace) and voltage (lower trace) for two different discharges. In Figure 8, the simultaneously measured light-pulse shape has been plotted. The same graph includes the measured instantaneous lamp power. As one would have expected for such short

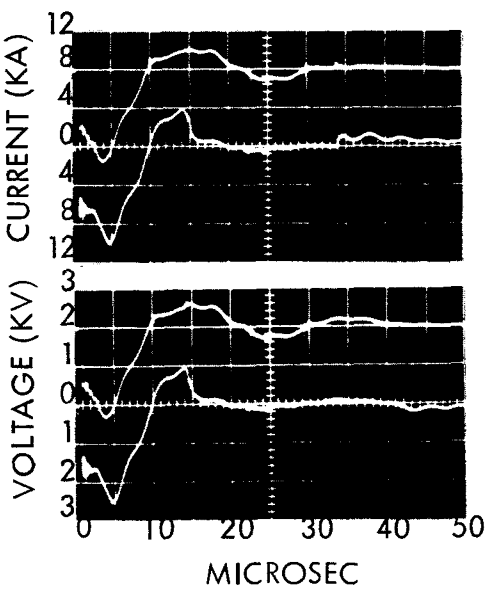

Figure 7. Two Samples of Measured Discharge Current and Voltage Across Ablative Lamp As a Function of Time

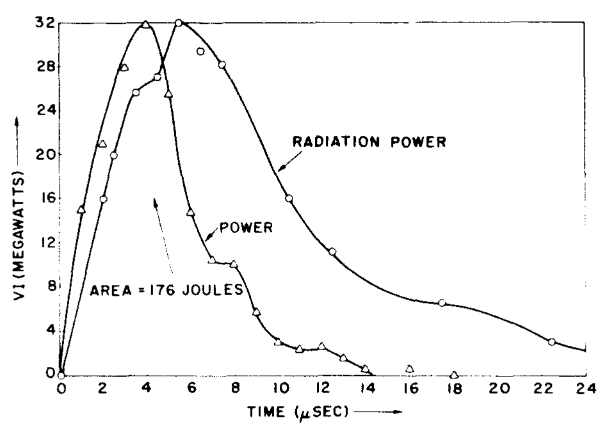

Figure 8. Instantaneous Lamp Power and Radiation Power (Relative Units) as Functions of Time

duration discharges, there is no straightforward relation between instantaneous lamp power and lamp radiation. The light pulse was recorded by a photodiode utilizing an S-4 response photocathode. From the measurements, it was found that for lamps operating at efficiencies of 20 percent or greater, average lamp resistance may be approximated in all cases by a simple formula:

$$R = \frac{\rho \ell}{A} \text{ ohm} \tag{12}$$

where

ρ = plasma specific resistance (ohm-cm)

ℓ = lamp length (cm)

A = lamp cross-sectional area.

Hence

$$= \frac{RA}{\ell} \tag{13}$$

From the data shown in the oscillogram (Figure 3), we find that the lamp geometry yields R = 0.25 ohms; A = 0.196 cm^2, and ℓ = 15.25 cm. Hence,

$$\rho = \frac{0.25 \times 0.196}{15.25} \approx 3 \times 10^{-3} \text{ ohm} \cdot \text{cm} \tag{14}$$

Using this value for lamp plasma resistivity, it is easy to find the near optimum ratio of circuit inductance to energy storage capacitance, namely

$$\frac{L}{C} \approx 10^{-5} \cdot \frac{\ell^2}{d^4} \text{ ohm}^2, \tag{15}$$

where lamp length (ℓ) and discharge channel diameter are measured in cm. Additional design equations are, of course, total discharge energy W_o and pulse duration τ. These are

$$W_o = 0.5C \; V_o^2 \tag{16}$$

$$\tau^2 \approx 10 \cdot LC. \qquad (17)$$

Combining Equations (16) and (17), one finds that

$$L \approx 10^{-3} \frac{\ell \cdot \tau}{d^2} \text{ henry} \qquad (18)$$

$$C \approx 10^2 \cdot \frac{\tau d^2}{\ell} \text{ farad} \qquad (19)$$

For the storage capacitance charging voltage,

$$V_o = \left(\frac{2W_o}{C}\right)^{1/2} \text{ volts} \qquad (20)$$

Therefore, solving Equations (18), (19), and (20), in the case of the lamp where

$\tau \approx 10^{-5}$ sec

$d = 0.15$ cm

$\ell = 20$ cm

$W_o = 250$ joules.

we get

$C = 1.1 \times 10^{-6}$ farad

$L = 9 \times 10^{-6}$ henry

$V_o = 2.1 \times 10^{-4}$ volts.

Although the above indicated values are optimum relative to electrical power transfer, deviations from the indicated circuit values by approximately one order of magnitude do not significantly affect lamp efficiency. For example, the lamp can be operated without loss in efficiency using a capacitance of 9×10^{-6} farad, a circuit inductance of approximately 1×10^{-6} henry, and charging voltage of 7.5×10^3 v.

2.2.5.2 Radiant Energy Distribution

The radiant energy distribution of the flashing light source as a function of time and wavelength is of greatest importance. To investigate this characteristic, a series of time-resolved semi-quantitative studies were performed with a special laboratory facility. A schematic of the apparatus used for these studies is shown in Figure 9. It consists of a stigmatic photographic spectrograph, a rotating mirror system, and imaging optics. The quartz lenses form a 0.1-cm diameter image of a selected spot of the lamp on the spectrograph entrance slit. A rotating plane reflector was placed in the light path in such a way as to cause image spot motion along the entrance slit. Because of the stigmatic image formation in the spectrograph, this procedure results in a 3-dimensional display of wavelength (horizontal axis), time (vertical axis), and radiance (photographic density) on the photographic plate.

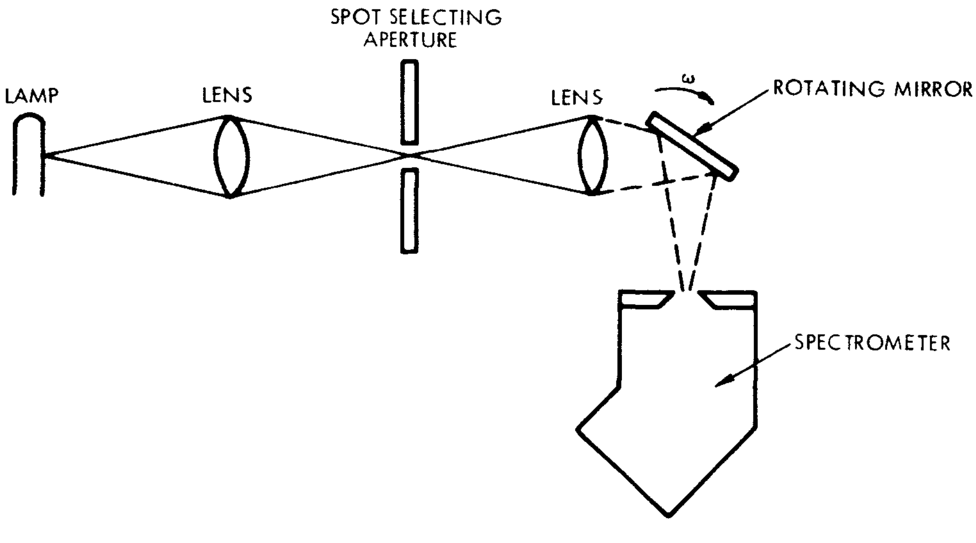

Figure 9. Schematic of Experimental Apparatus for Performing Quantitative Time Resolved Spectroscopy (Time Resolution ~ 1 μsec; Wave Length Resolution ~ 0.5 Å)

Figures 10 and 11 show two examples of photographic plates obtained in this way. Figure 10 shows several adjacent spectral ranges with mercury and neon reference spectra for wavelength identification. Figure 11 shows three time-resolved spectra of Pyrex lamp radiation, when discharge energy = 250 J, initial air filling = 1 mm Hg, and wavelength interval = 2,800 to 3,600 Å (a TRW Instruments image converter camera was used to photograph the spectrum. Time increases downward, showing the first 25 μsec of the discharge. Interesting features include the intense continuum down to the Pyrex cutoff, an Si III doublet (3, 093 to 3,096 Å) which changes from emission to absorption during the discharge, a strong B II line (3,451 Å), and weaker lines due to Si IV and 0 III. The lower spectrum is of a mercury reference source. Table I lists the more significant conditions of the test.

Time resolution was 1 μsec. The spectroscopic study yielded the following data:

1) During the ignition phase (approximately 1 μsec) a line spectrum is generated, which after approximately 1 to 2 μsec is completely dominated by silicon lines. This supports the assertion that the origin of the emissive lamp plasma is the quartz lamp walls. Lines from the initial filling gas are only significant during the first μsec of the discharge.

2) Approximately 1μsec after ignition, a rapid buildup of a continuous spectral energy distribution commences. Continuous emission prevails during the remainder of the discharge. This continuum extends over the total investigated range of from 0.25 to 0.65 μsec.

The spectral apparatus used in this study is capable of measuring the absolute radiance distribution as a function of wavelength and time, but because of the time limitations, was not employed as such.

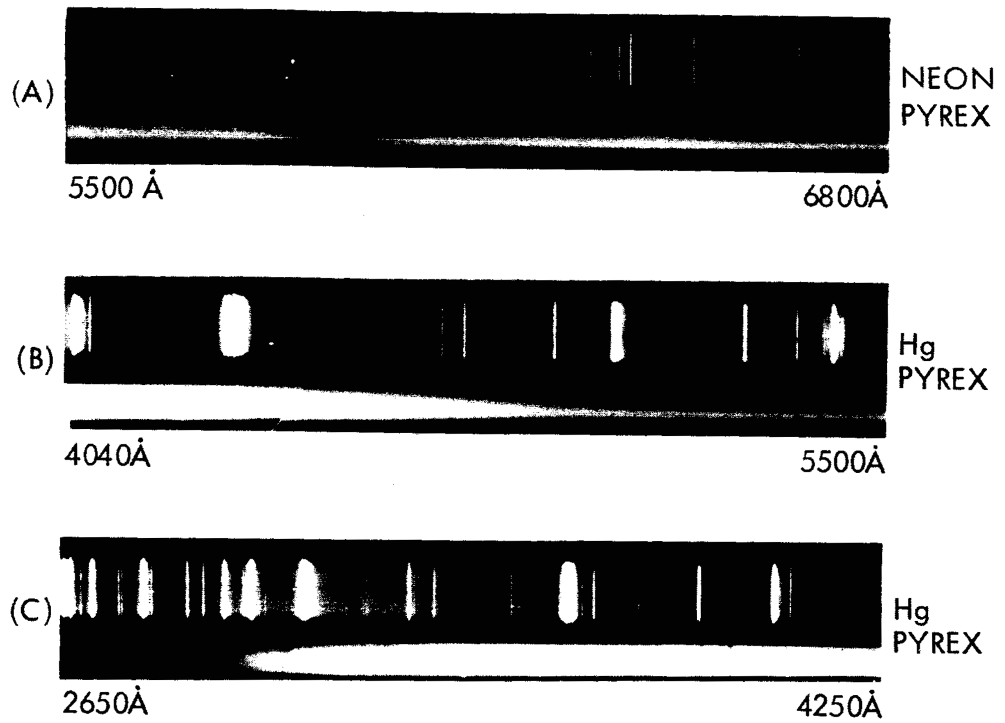

Figure 10. Time-Integrated Photographic Spectrum of Pyrex Ablating Lamp for Adjacent Spectral Regions

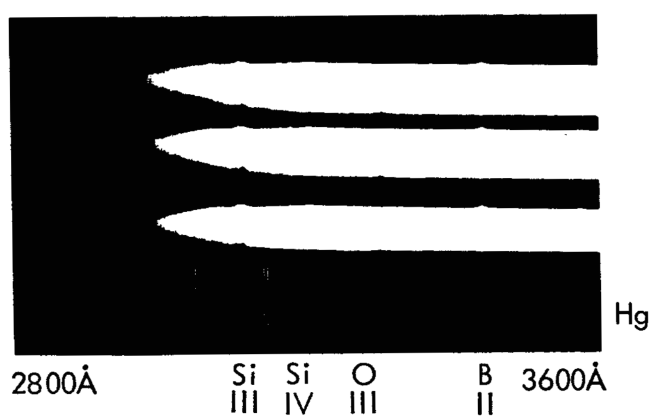

Figure 11. Time-Resolved Photographic Spectrum of Quartz Ablating Lamp.

Table 1. Conditions of Radiant Energy Distribution Test

X (mm)	Relative to	λ	Identity	Intensity	Remarks
-2.9	3125.7 Hg	3093	Si III E_ℓ = 18ev	10	Switches to absorption
-4.0	3125.7 Hg	3086	Si III E_ℓ = 18 ev	10	
+6.0	3131.8	~3992	Si II 3199 - 3193 -3188	10	Maximum of broad (~100 Å) emission region
+11.0	3341.	3451	B II	20	
-4.0	3341	3301			Absorption
+3.3	3131.8	3165	Si IV	5	Relatively
-7.6	3341	3265	0 III	air	Very narrow
-8.0		3261	0 III	air	Disappears quickly

2.2.5.3 Radiant Lamp Efficiency

Radiant lamp efficiency was determined for a number of different lamp geometries as a function of total electrical input energy, and for different electrical circuit parameters (at fixed input energy and lamp geometry). As mentioned previously, total lamp efficiency was practically independent of circuit capacitance (lamp geometry and total input energy fixed). However, radiant lamp efficiency depends very critically on both geometry and input energy.

A schematic of the apparatus used to measure radiant efficiency is shown in Figure 12.

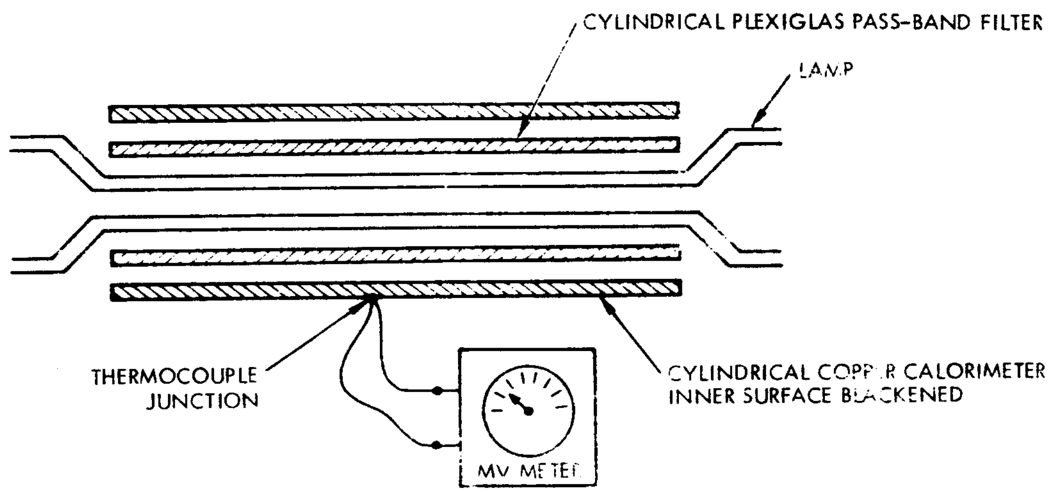

Figure 12. Schematic of Measuring Apparatus for Determining Absolute Radiative Lamp Output Energy

The lamp was mounted in a hard vacuum system. The quartz tube was surrounded by a plexiglass tube which acted as a passband filter to select the wavelength range $0.355\ \mu$ - $1.1\ \mu$ for measurement. The plexiglas tube was enclosed by a copper calorimeter which had a black absorbing coating applied to the surface facing the discharge. The absorbed radiative energy raised the copper calorimeter temperature by an increment ΔT, which was measured with a copper-constantan thermocouple junction. Total radiative energy, J, is calculated from the measured ΔT by the relation

$$J = C'W \, \Delta T \tag{21}$$

where

W = calorimeter weight (gram)

C' = specific heat of copper (joules/gram ^{o}K)

By operating the measuring system in a hard vacuum, heat convection to the calorimeter was eliminated. Also the cooling time-constant is increased significantly, allowing particularly accurate measurements. It should be noted that the radiative energy measurements were made entirely on a calorimetric basis which is significant for data reliability and accuracy.

The results of these measurements are plotted in Figure 13.

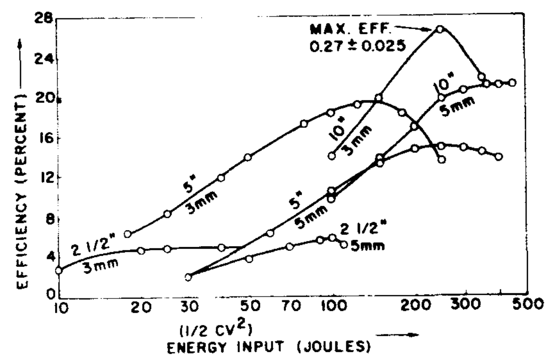

Figure 13. Calorimetrically Determined Quartz Ablative Lamp Efficiency as a Function of Electrical Input Energy and Lamp Geometry. Wavelength Range, 0.355 μ to 1.1 μ

Efficiencies have been defined as

$$\eta = \frac{J}{0.5\, C V_o^{\,2}} = \frac{C'W}{0.5\, C V_o^{\,2}} \cdot \Delta T \tag{22}$$

Maximum efficiency for a 250-joule input lamp has been determined as 0.25 ±0.025 for a lamp geometry of 10-in. electrode spacing and a capillary diameter of 0.3 cm.

2.2.5.4 Radiant Energy Repeatability

It has long been known that all types of ablative lamps show very consistent repeatability of light output from shot to shot. This characteristic can probably be related to the lamp's principle of operation. Because ablation occurs constantly, the lamp bulbs are in effect self-cleaning and never decrease in transparency. Also, because each flash generates a fresh supply of carrier gas, plasmas of identical composition are used repeatedly. In conventional high-power sealed-off lamps, each lamp flash actually changes the carrier gas somewhat. Figure 14 shows the results of two ablative lamp tests where 100 consecutive flashes were superimposed on a single oscillogram. Excellent reproducibility is demonstrated in both experiments. The oscillograms show the current pulses generated from an S-4 response photodiode.

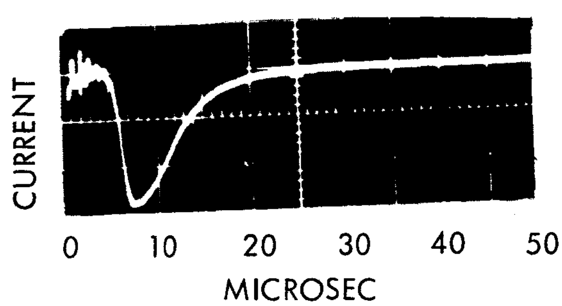

Figure 14. Oscillograms Showing 100 Superimposed Consecutive Current Pulses From an S-4 Response Photodiode Excited by the Quartz Ablative Lamp Radiation

2.2.5.5 Life Tests

A life test was conducted on a 20-cm long, 0.3-cm diameter lamp mounted in a hard vacuum and thermally insulated from its mounting structure. Thus, there was no effective cooling of the lamp by conduction. The lamp was operated continuously at a flash rate of one flash per sec and 250 joules input per flash. Hence, average lamp input power was 250 w. Light output was continuously monitored by an S-4 response photodiode. A counter registered each flash. The result of the test is plotted in Figure 15.

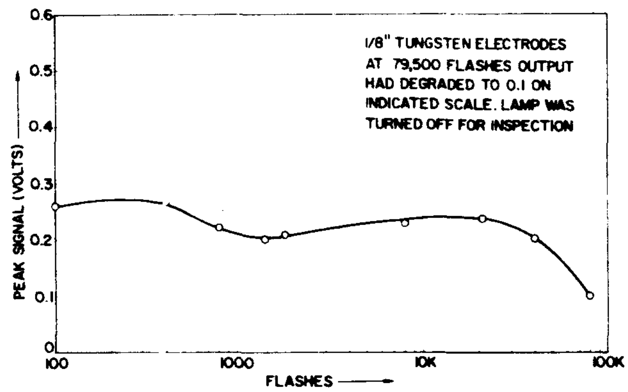

Figure 15. Peak S-4 Photodiode Response Signal as a Function of Number of Flashes. Lamp Length, 20 cm; Lamp Diameter, 0.3 cm; Input Energy, 250 Joules; Flash Rate, 1 Sec

Because of severe degradation of the light output after approximately 80,000 flashes (22-hr continuous operation), the system was disassembled and inspected. It was determined that the reason for the light degradation was lamp-bulb darkening. This, in turn, was caused by ablation products (SiO_2) clogging the exhaust. The exhaust mechanism, vital for keeping the lamp clean, ceased to be effective and rapid decrease of lamp output resulted. Although this problem has not yet been entirely overcome, it is believed that it can be eliminated by a redesign of the electrode structure and the exhaust port.

2.2.5.6 500-Watt Life Test

The same lamp tested at the 250-w average input level was (after cleaning) again tested at the 500-w input level (250 joules per pulse and 2 pulses per sec). Again the lamp was tested in a hard vacuum and was thermally insulated from the mounting structure.

The SiO_2 condensation problem which was encountered in the 250-w test after 22 hr became apparent after approximately 10 hr of continuous operation at 500 w. At this input level, although the lamp structure was red hot, it did not affect the operation of the lamp.

2.2.5.7 Thermal Vacuum Test

The purpose of these tests was to establish lamp starting capability and to determine if mechanical damage occurred due to mechanical stresses under cold-temperature conditions.

A copper shroud was placed around the lamp structure within the high-vacuum chamber of the test fixture shown in Figure 3. Liquid nitrogen was circulated in the copper tubing lining the shroud until the temperatures at the lamp structure had stabilized at $-55^{\circ}F$. Normal starting procedures were then instrumented to fire the ablative lamp.

Results:

(1) The lamp operated normally; slightly more boiler power was required to set the main chamber pressure levels to the firing point.

(2) No structural damage was noted.

(3) After initial firing, the boiler was not required for lamp operation.

(4) The lamp was turned off after operating 5 minutes and then restarted. Operation was normal.

2.2.6 Thrust Phenomenon

Average thrust levels which can reasonably be expected from quartz ablative lamps are so small as to render exact measurement very difficult. The following estimate may serve to show this. For isentropic expansion of exhaust gas through a nozzle, gas exit velocity is:

$$\bar{v}_x^2 = \Phi^2 \cdot \frac{k}{k-1} \cdot \frac{2RT_c}{\bar{\mu}} \text{ cm}^2/\text{sec}^2 \tag{23}$$

where

Φ = 0.9 maximum nozzle efficiency

$k = c_p/c_v$

$c_p; c_v$ = specific heats at constant pressure and volume, respectively

$R = 8.31 \times 10^7$ erg/mol ^oK

T_c = stagnation point gas temperature

$\bar{\mu}$ = mean gas molecular weight

Net composition is Si + 20 for a fully dissociated gas, i.e., $\bar{\mu} = 20$; for ideal gas $k = 5/3$; $k/k-1 = 5/2$; $T_c = 2 \times 10^4$ ^oK $\quad \bar{v}_x = 5.8 \times 10^5$ cm/sec

At a lamp flash rate of 1 per second average mass flow $m = 10^{-4}$ gr/sec. and hence average thrust $\dot{m}\bar{v}_x = 0.58$ dyne

The indicated thrust is obviously the maximum thrust which could be obtained had the lamp been outfitted with an expansion nozzle and if all the gas could indeed be expanded through the nozzle. In practice, however, the exhaust system is an elongated tube. As a result the exhaust gas temperature is in the vicinity of 500^oK, furthermore, most of the cooling lamp exhaust gas is highly condensable and precipitates as SiO_2 and Si with just a small amount of oxygen escaping. The effective exhaust gas mass is estimated to be much less than 0.1 of the total. Condensation of SiO_2 and Si in the exhaust system is amply evidenced in the investigated lamps. The combined effect reduces expected thrust to values below 5×10^{-3} dynes, which is equivalent to approximately 50 micropounds average thrust. In view of the fact that this thrust is very small, a direct measurement would have been too costly an undertaking within the scope of the contract.

2.2.7 Thrust Negator

Since the lamp exhaust directly into space, a relatively simple thrust deflector can assure zero net thrust. The design should assure isolating surrounding equipment from the exhaust and preventing material condensation on the deflector. A suggested approach to the design of such a thrust negator is shown in Figure 16.

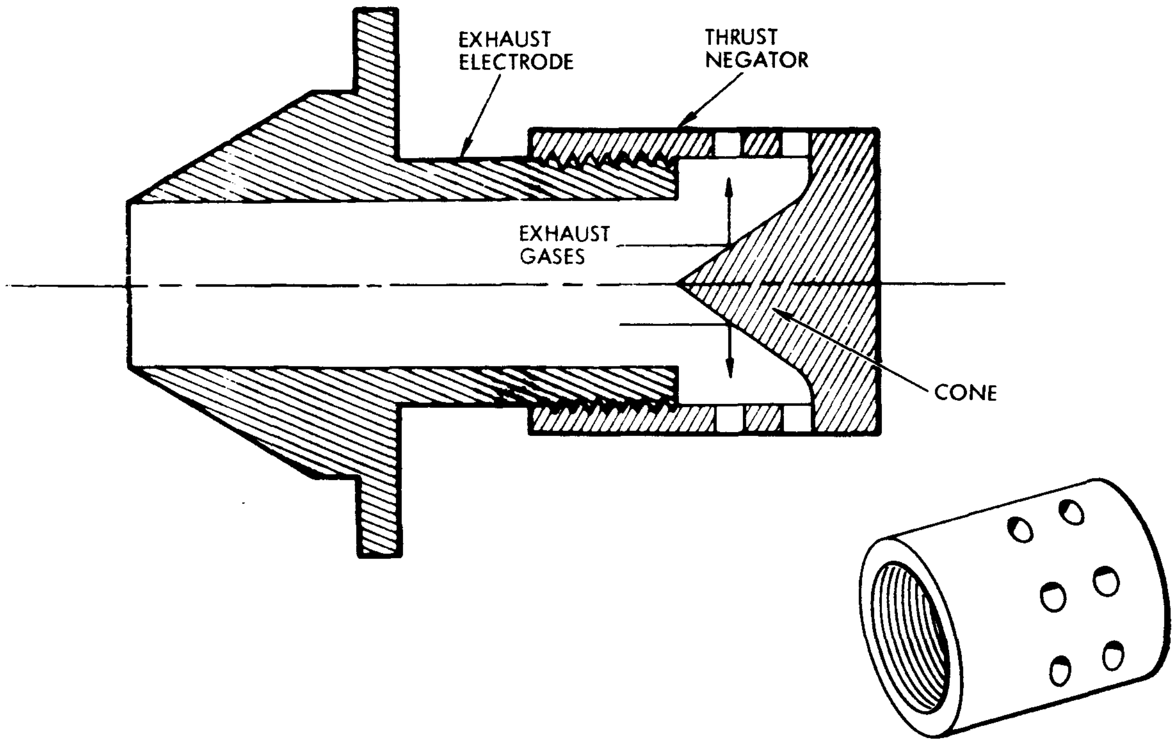

Figure 16. Thrust Negator

2.3 PULSED-ABLATOR CONCEPT

2.3.1 General

This approach to the design of the ablative lamp was explored extensively but abandoned in favor of what was considered the superior "boiler approach." The work performed on the pre-ablator system is generalized and described here for information purposes. In this lamp concept a low energy pre-ablative chamber supplies material to the main chamber to initiate the gaseous discharge in short duration pulses. The main chamber flashes each time a pre-ablator injects a quantity of material into it. A significant point of the operation is that the pre-ablator supplies only enough material to initiate the energy discharge. The material required to sustain the main discharge is supplied from actual ablation of the quartz walls of the main chamber.

A diagram of a pulsed-ablator type lamp and a schematic of its associated electronics are shown in Figure 17.

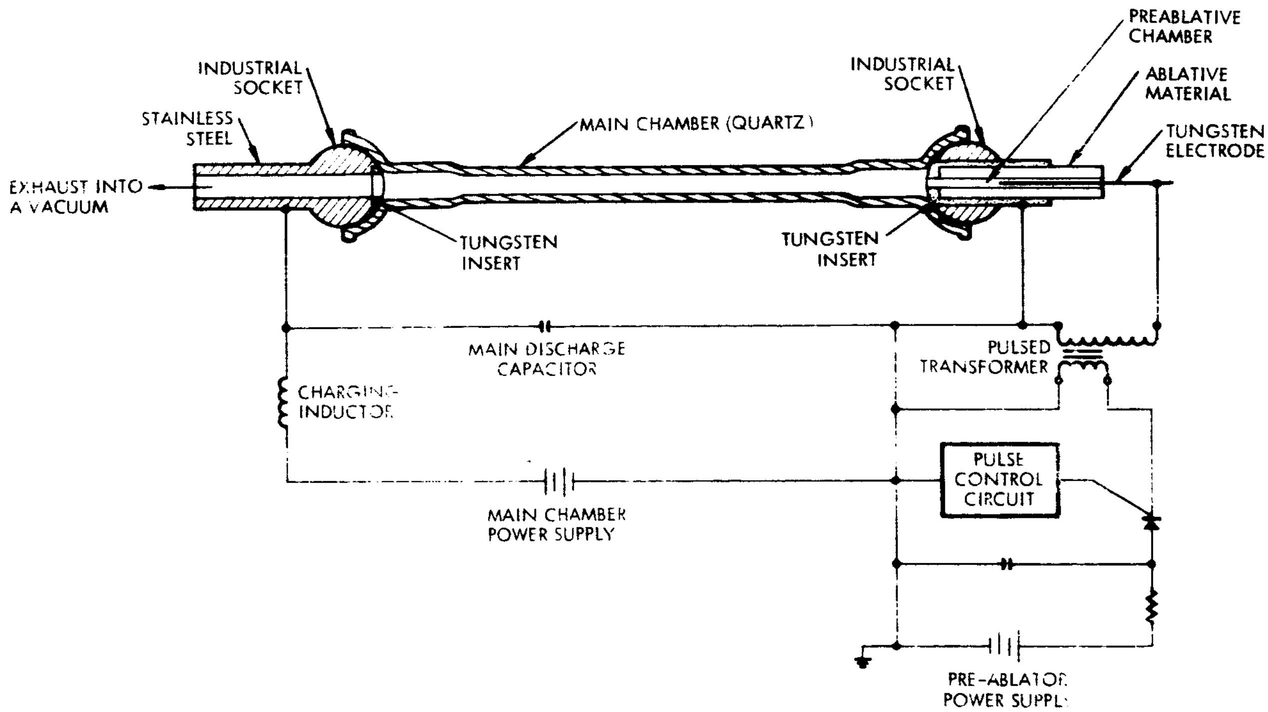

Figure 17. Block Diagram and Schematic of Pulsed-Ablator Lamp

2.3.2 Functional Description

Initially, the environmental conditions in the main chamber are a vacuum of $\approx 10^{-5}$ mm of Hg and a temperature of 25°C. The main chamber capacitor is charged and connected directly to the two ball joint electrodes. The high voltage is held off from discharging the main chamber capacitor by the low internal pressure. When a high voltage pulse is applied to the pre-ablator electrodes, a creeping arc is generated along the inside surface of the ablative material between the center tungsten electrode and the common ball joint electrode. This arc generates a quantity of gaseous material by ablating the pre-ablator sample. The gaseous material then flows into the main chamber because of its near vacuum state, and causes a rapid rise in the main chamber pressure. This pressure follows the Paschen curve (Figure 18), and rises to the voltage level of the main capacitor, at which time the main discharge occurs. After the capacitor has discharged, the main chamber is exhausted to a low pressure again. The main chamber capacitor charges through the charging inductor, and the cycle is repeated each time the pre-ablator is pulsed.

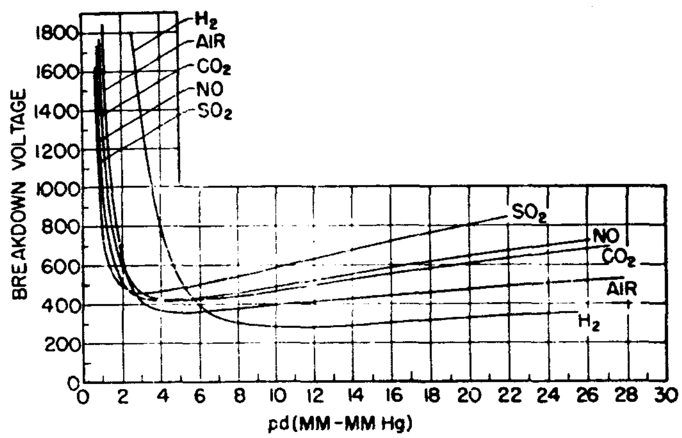

Figure 18. Paschen Curves for Various Gases*

This lamp design has two very attractive features. The first is that the lamp itself is used to switch the main energy discharge. The voltage on the main burner is applied directly from the capacitor, eliminating the need for a power switching element. As the peak power in the main chamber can be in excess of 5 megawatts, this is a significant advantage. The second advantage is that the pre-ablator supplies material only in short bursts of approximately 10 μsec duration. Since the repetition rates are only 1 pulse and 32 pulses/sec, the duty cycle is extremely small. The result is that for the duration of the pulse, the material generation rate can be very high without an appreciable average rate of material usage. The fast rate of material generation during the

*M. Knoll, F. Ollendorff, and R. Rompe, "Gasentladungstabellen," p. 84, Springer-Verlag OHG, Berlin, 1935.

pulse allows pressures in the main chamber to be sufficiently high to be able to operate with an open exhaust port. This results in maximum cooling and eliminates any chance of the exhaust opening becoming plugged. In addition, the control circuitry to control the firing rate is of a relatively low power level.

2.3.3 Design Features

In the investigation of the pulsed-ablator concept, two main areas required considerable effort:

1) Type of ablative material to be used in the pre-ablator
2) Location of the pre-ablator with respect to the main chamber.

2.3.3.1 Type of Pre-Ablator Material

With respect to the type of ablative materials in the pre-ablator a study to be used was made of the following:

1) Dupont SP-1 Polyimide
2) Plexiglas
3) Teflon
4) Hystl
5) High temperature epoxy material

In the early phases of the program, lamp operation was better when the pre-ablator was in close proximity with the main chamber. However, the high operating temperature of the main chamber (600°C) dictated that a high temperature material be used in the pre-ablator if it was to be close to the main chamber. Since the DuPont material could be operated at a temperature of 700°C, it was used initially. A problem developed with this material, however, that prevented its eventual use. When an arc was repeatedly struck across its surface, a conductive carbon path always formed between the two electrodes and prevented any further arc discharges. Thus, ablative action would cease.

Teflon was employed with partial success, although its maximum temperature capability of approximately 300°C necessitates some isolation from the main chamber. Its main disadvantage is that the gases resulting from its ablation attack both the quartz main chamber and the electrodes.

Plexiglas was also evaluated but showed little advantage over Hystl.

The epoxy material was unsatisfactory due to the rapid generation of carbon along the discharge path and a consequential inability to produce an arc discharge.

The most promising material investigated was Hystl. This material can operate up to 300°C, which allows for reasonable mechanical constraints. This material did not develop carbon on the ablative surface as a result of the arc discharge. In addition, there is no oxygen in its structure. Analysis of the electrodes indicated that oxygen in the ablative gases was a main cause of electrode deterioration.

2.3.3.2 Location of Pre-Ablator

The location of the pre-ablator with respect to the main burner was influenced by the following conditions:

1) It must be thermally isolated.
2) The closer it was to the main burner, the easier it was to control main burner firing.
3) The closer it was to the main burner, the more pronounced was the effect of "flash-back" on the ablative sample.

The main problem with most materials used was that a conductive carbon path formed between the electrodes preventing arcing. The carbon path seemed to form easily with a "soft discharge". When the ablative sample was very close to the main burner, the flash-back from the main burner kept the discharge path clean and free of carbon. However, the rate of burning of ablative material by the main chamber was so rapid under these conditions that unsatisfactory lifetime resulted. An attempt was made to produce a higher temperature in the pre-ablator independent of the main chamber by adding a capacitor dumping circuit to the existing pulse circuit. This allowed the pre-ablator to be isolated from the main chamber, but still permitted for clean operation of the pre-ablator chamber. This method improved the pre-ablator performance. However, it represented a considerable increase in the complexity of the electronics.

2.3.4 Power Supplies

The pulsed-ablator method requires three power supplies:

1) Pulse triggering supply
2) Pre-ablator capacitor supply
3) Main chamber supply

The triggering and pre-ablator capacitor supplies together control the firing of the pre-ablator. The capacitor dumping circuit C_1R_1 provides the low impedance source necessary for a high current discharge. Details of the circuitry are shown in Figure 19.

The main chamber power supply requirements are basically the same as for the boiler method except that no triggering circuitry is required. The only additional requirement is a delay circuit in the capacitor charging line to assure extinguishing of the main discharge.

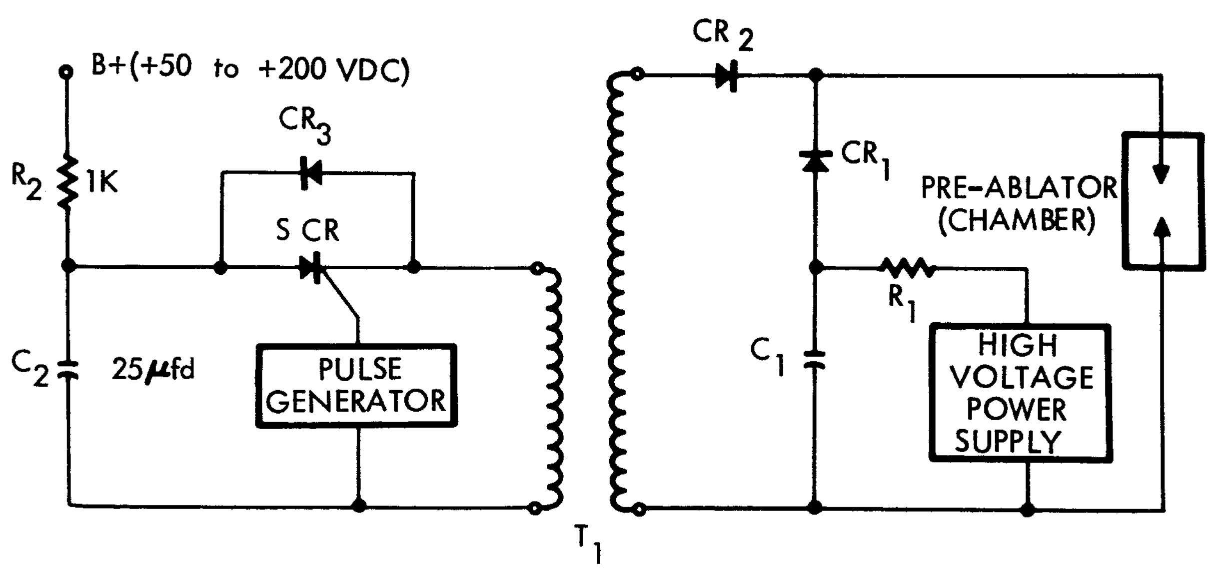

Figure 19. Pulsed-Ablator Power Supply Circuits

3. PARTS LIST

In accord with Article XII of Contract NAS 9-5374, the following data are furnished. Parts indicated in Figures 1 and 19 of this report and special materials are identified below.

	Description	Mfg Part No.
	Figure 1	
V_1	Tube	2021 General Electric
V_2	Tube	5022 General Electric
Ignitron	Ignitron	7171 General Electric
L_1	50 μh Inductor	UTC
T_1	Transformer	UTC No. H49
T_2	Transformer; primary-shield secondary-centershield	L98 Hypersil Core 2" x 3" window 5/8" x 1" core 15 turns of RG9 cable
	Figure 19	
SCR	2N2575	Motorola
CR1	25 k v Diode	SCH 25000 Semtec Corp., Newbury Park, Cal
CR2	25 k v Diode	SCH 2500 Semtec Corp., Newbury Park, Cal
CR3	Diode HF50137	Hughes Semiconductor
C_1	0.005 at 7 kv	No. LSG502-7M Condenser Products Capacitor
R_1	50 K at 20 watt	Ohmite Corp., STK No. 1836
R_2	1 K at 50 watt	Ohmite Corp.
C_2	25 μfd 2500 v	PQ 2525 Sprague
T_1	250:1 Autotransformer	TRW design
Pulse Generator		PARABAM - waveform generator model W2
High-voltage power supply		TRW design

Materials

(1)	Optical Quartz	Westglass Corp., El Monte, Cal.
(2)	Plexiglas	Fry Plastics, Los Angeles, Cal.
	HYSTL	TRW formulation
	Teflon	E. I. Dupont
	Dupont SP-1 Polyimide	E. I. Dupont, Chemical Division
	Epoxy materials	TRW formulation
(3)	Tungsten	
	1% thoriated (AWS-ASTM: EWth 1)	Sylvania
	2% thoriated (AWS-ASTM: EWth 2)	Sylvania
	Mallory 1000	Ducommon
	Tantalum	Ducommon
	PURETUNG (AWS-ASTM: EWP	Sylvania

4. NEW CONCEPTS

During the period of this report no new technological concepts were developed by TRW as a result of the work performed under Contract NAS 9-5374.